Development of a Tool Temperature Simulation During Side Milling

Thorsten Helmig[1](✉), Hui Liu[2], Simon Winter[1], Thomas Bergs[2], and Reinhold Kneer[1]

[1] Institute of Heat and Mass Transfer, RWTH Aachen University, Aachen, Germany
helmig@wsa.rwth-aachen.de
[2] Laboratory for Machine Tools and Production Engineering, RWTH Aachen University, Aachen, Germany

Abstract. Current modeling approaches of cutting processes require on the one hand extensive numerical and analytical simulations and further an experienced user in the field of numerical simulations, which makes a large-scale application time-consuming to apply.

Therefore, the goal is to implement existing models into an established side-milling simulation program aiming for a computationally fast and user-friendly simulation approach capable of predicting transient tool temperatures along the cutting edge. Aim of this work is the development of the thermal model, which can later be implemented into existing programs. The model process involves the following two major steps: First, a geometric engagement simulation of the milling process with a parameterizable tool geometry is performed. These results are used to form a database linking the specific cutting force components with the heat flux components. Second, a three-dimensional transient heat conduction model of the cutter is established, applying the calculated heat flux components as boundary conditions in the simulation. Finally, first results of the performed simulation are presented and evaluated, in particular to validate the work flow and user accessibility. Future studies will then focus on further parameter analysis and experimental validation.

Keywords: Transient Thermal Modeling · Side-milling · Finite-Element-Method

1 Introduction

During milling, almost ninety percent of the used mechanical energy is converted into heat [1]. Part of this thermal energy is transferred from the cutting zone to the tool and the toolholder, resulting in three-dimensional temperature fields and gradients. In turn, thermal stresses arise inside the tool, which accelerate the thermo-mechanically induced tool wear on the one hand. On the other hand, the thermal distortion can lead to a displacement of the tool center point and thus to a reduction in machining accuracy. Therefore, understanding the heat partition in the cutting area and the development of tool temperature plays an important role not only in scientific research, but also in applied manufacturing processes.

S. Ihlenfeldt (Ed.): ICTIMT 2023, LNPE, pp. 308–317, 2023.
https://doi.org/10.1007/978-3-031-34486-2_22

In milling, the estimation of the tool temperature by the given cutting has been investigated with comprehensive experiments in the last decades. Depending on the experimental approach, the investigations so far can be divided into local temperature measurements [2–6] and thermography-based temperature field measurements [7–9]. Local temperature measurement can be for example obtained by using a thermocouple or fiber optic cable connected to a pyrometer. To mount the sensor, a hole is usually drilled in the tool up to the measuring point by means of wire electro-discharge machining. A drawback of local temperature measurement is that it cannot provide information about temperature gradients, or the resulting temperature field. In contrast, Infrared Thermography yields spatially resolved temperature data, but only intermittent optical access of the tool surface is given due to the rotation of the milling tool and the evolving chips. Consequently, comprehensive temperature measurements during machining are challenging to acquire.

In order to reduce the amount of experimental effort and to support thermal analysis, modeling approaches come into focus. A popular analytical approach for orthogonal cutting processes is the use of superposition by Greens function to estimate the temperature field [6]. However, this approach is limited to comparable simple tool geometries and heat flux distributions. As an alternative, numerical methods can be used, as these can handle advanced (tool-) geometries and heat flux distributions along the tool surface and provide transient temperature fields as an output. In turn, the obtained temperature fields can be used in post-processing to estimate heat fluxes into the machine tool, ultimately leading to a shift in the tool center point (TCP). Hence, this work aims for the development of a novel numerical approach to estimate the transient temperature field of a milling tool by resolving the spatially varying and transient heat flux. The heat flux caused by the manufacturing process is a-priori calculated by a Finite-Element simulation and later used as input for the boundary condition in the thermal simulation. By using pre-calculated heat source terms, the simulation time of the process can be significantly reduced, allowing for faster and application-oriented studies.

2 Overview Workflow

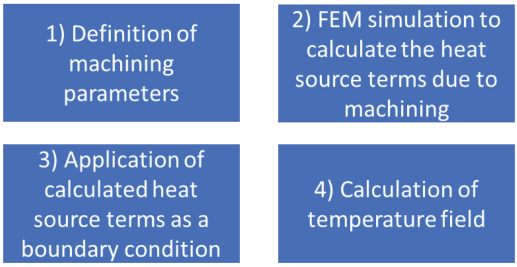

Fig. 1. Workflow to calculate a transient milling tool temperature field.

For an improved understanding of the overall procedure, Fig. 1 highlights the workflow.

In a first step the considered machining parameters are defined. The parameters are then used in a FEM simulation of the milling process to calculate the heat source terms. These are summarized in integral value and are later applied as a boundary condition in the thermal simulation of the tool. The heat source term is homogeneously distributed along the engaging cutting edge, which will be explained in the next section.

3 Tool Geometry, Mechanical and Thermal Modeling

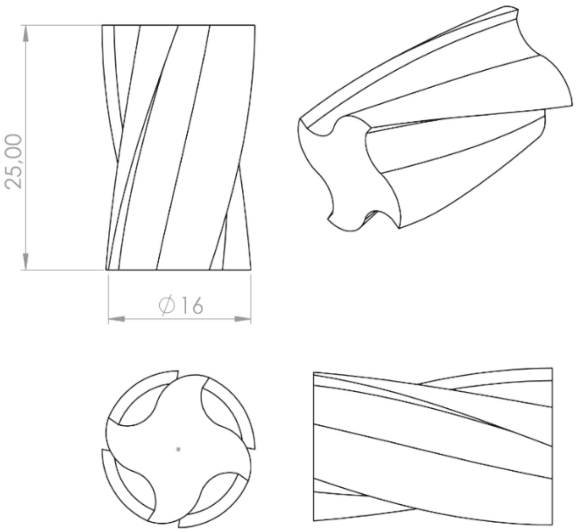

Fig. 2. Geometry of the modelled milling tool.

The considered tool for simulation is a solid carbide milling cutter from Sandvik Coromant, type 2P342–1600-CMA 1740. The geometry of the milling cutter is shown in Fig. 2. The flute helix angle of the tool is 38°. In a first step, the tool is not resolved in its entirety, but up to a height of 25 mm.

To estimate the heat flux into the tool, three-dimensional chip formation simulations of the milling process are performed. The simulation uses a Coupled Eulerian-Lagrangian (CEL) approach, where the workpiece is defined in the Eulerian domain and the tool in the Lagrangian domain. The tool is considered as a rigid body neglecting wear effects. The workpiece material under study is AISI 1045. The Johnson Cook material (JC) model is used to describe the thermo-viscoplastic behavior of the workpiece. The JC model consists of three multiplied terms that describe the influence of strain, strain rate and temperature:

$$\sigma_F = \left(A + B \cdot \varepsilon^n\right) \cdot \left(1 + C \cdot \ln\left(\frac{\dot{\varepsilon}}{\dot{\varepsilon}_0}\right)\right) \cdot \left(1 - \left(\frac{T - T_0}{T_m - T_0}\right)^m\right)$$

The model parameters for AISI 1045 are inversely calibrated in the previous work and used in this study, as shown in Table 1.

Table 1. Model parameters of the Johnson Cook material model for AISI 1045

A	B	C	m	n	T_m	T_0	$\dot{\epsilon}_0$
[MPa]	[MPa]	-	-	-	[°C]	[°C]	s^{-1}
541.5	460	0.004	0.05	1.047	1460	20	1

The simulations are performed in the commercial software ABAQUS version 2021. Figure 3 gives an overview of the simulation domain. The increase in internal energy of the tool at one revolution is used to estimate the heat source applied in the subsequent thermal analysis.

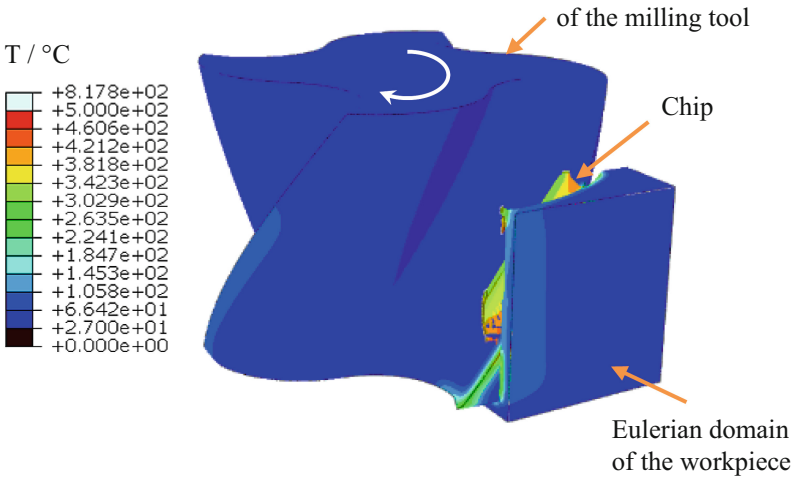

Fig. 3. Chip formation simulation of the milling process based on the coupled Eulerian Lagrangian method.

After the mechanical simulation, the thermal analysis is performed. To transfer the tool geometry into a thermal model, a Finite-Volume-Approach is chosen. The implementation is performed in a MatLab environment. The governing equation for a three-dimensional transient heat conduction problem with constant density ρ, heat capacity c_p and heat conductivity k reads:

$$\rho c_p \frac{\partial T}{\partial t} = k\frac{\partial^2 T}{\partial x^2} + k\frac{\partial^2 T}{\partial y^2} + k\frac{\partial^2 T}{\partial z^2} + \dot{q}'''(x, y, z, t)$$

Further, a heat source term $\dot{q}'''$ is located on the right-hand side, to consider the heat flow into the tool during machining. The values of the thermophysical properties are shown in Table 2:

Table 2. Thermophysical properties of the tool.

Property	Value
Density	14800 kg/m^3
Heat Capacity	243 J/kg K
Heat Conductivity	81.78 W/mK

As outlined in the previous section, the workpiece and chip formation are not resolved in the thermal simulation of the milling tool. Instead, the machining of the workpiece and chip formation is resolved by the FEM approach. The results of the FEM approach are then used to calculate an integral heat source value (Table 3), which is then homogeneously distributed along the engaging cutting edge (Fig. 4).

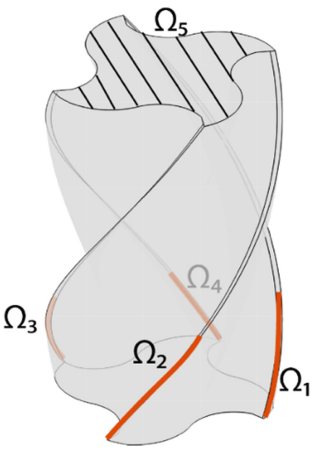

Fig. 4. Tool geometry with applied boundary conditions. For boundaries 1–4 a heat flux boundary is applied, while the tool top is set adiabatic. The sides of the tool and the bottom are set adiabatic but not particular highlighted here.

Along the boundary segment $\Omega_1 - \Omega_4$, the heat source term caused by the cutting process is applied up to a height of 7.5 mm. As the cutting tool is rotating during machining, the heat flux is not applied at all cutting edges simultaneously, but rather one cutting edge after another. An example sequence of one cutter revolution is shown in Fig. 5, highlighting that only one cutting edge engages at any timestep. Further, the applied heat source term is the same the for every cutter rotation. Due to the helix angle, the heat source is expected to move along the cutting edge during the engagement.

However, a spatially constant mean heat source is assumed in this work for two reasons: First, the focus is to establish and test the overall simulation workflow. Therefore, the model is built with the most essential parameters in order to eliminate possible sources of error in the development and ensure a stable model. In the future, the model is extended step by step to ensure a high stability for the later application in manufacturing environment. Next steps certainly include spatially varying heat source terms, convective heat transfer by cooling fluid. However, for now the heat source term is assumed to be constant along the engaging contact edge.

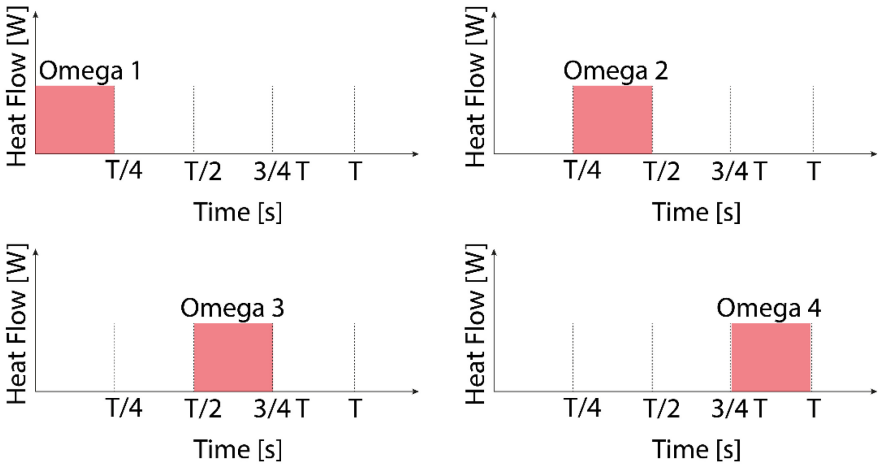

Fig. 5. Example of the applied heat source for the engaging cutting edges. The four cutting edges engage consecutively one after another.

Regarding further boundary conditions, the top of the tool is set adiabatic (Ω_5). Consequently, heat flux from the tool into the machine structure is not considered yet, but will be focused in future work. Due to the adiabatic boundary at the top, the tool temperature tends to be slightly overestimated. This will be particular noticeable for longer simulation times. For future studies, the boundary Ω_5 will be enhanced to consider heat flow into the machine tool. The remaining faces at the side and the bottom of the tool are also set to an adiabatic boundary condition, however not particularly highlighted here. As the sides can be selected as an independent boundary, convective cooling due to the use of cooling lubricant or contact heat transfer at the chip-tool interface can be considered. Finally, the effect of tool wear is integrated implicitly in future studies. As for a worn tool surface an increase in generated heat is expected, the boundary heat source terms can be adjusted accordingly.

After establishing the model, three different test cases with varying feeds are investigated to analyze the impact on the temperature field. The varied parameters are shown in Table 3:

Table 3. Test Cases and corresponding cutting parameters

Test Case	Cutting Speed v_c [m/min]	Feed f [mm]	Cutting Width a_e [mm]	Cutting Depth a_p [mm]	Power W]
1	100	0.1	2.5	7.5	175.291
2	100	0.2	2.5	7.5	219.102
3	100	0.3	2.5	7.5	256.97

4 Results

Figure 6 shows local temperature trends from Test Case 1. The location of extracted local temperature data is shown in the right sub-image. The measurement spot is located not directly at the cutting edge where the heat source term is applied, but a few cells below the surface. Further, the first ten revolutions of the cutting process are visualized.

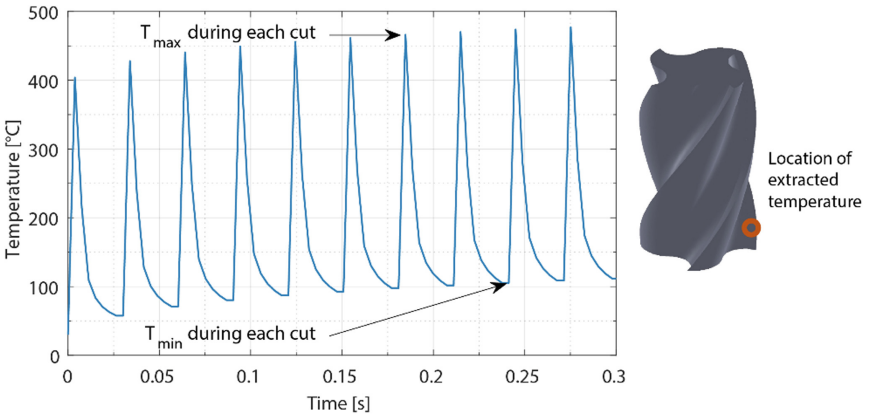

Fig. 6. Results of Test Case 1 during for the first 0.3s. The minimum and maximum temperature during each cut are highlighted.

In general, an oscillating behavior is observed. With a cutting speed of 100 m/min and a cutter radius of 8 mm, a cutting edge engages each 0.03 s, which corresponds well with the observed temperature oscillation. The engagement causes a fast increase in temperature, however followed by a rapid fall as the heat spreads into the tool. However, the temperature does not fall back to its initial value, but starts slightly higher as the next cut is already performed. In the long term, the entire tool will heat up. Of course, such temperature trends need an experimental validation, therefore a measurement setup with a high temporal resolution is required in order to resolve the occurring transient temperature trends. Previous studies applied a pyrometer to resolve such fast processes [10]. A similar approach is intended in the future, but requires comprehensive planning and layout of the experimental setup.

To get an overview of the temperature development during longer processing times, the maximum, minimum and mean temperature for each cut is calculated. The results are shown in Fig. 7, visualizing a fast increase in all depicted temperatures at the beginning. Afterwards, a transition into a linear trend for all three shown temperatures is observed. Further, due to the heat spreading and fast decrease in temperature, the mean is rather oriented towards the minimum than to the maximum value. The orientation of the mean value towards the minimum is maintained throughout the entire investigation time. The maximum temperatures approach a level of 600 °C after 5 s. In contrast, the time averaged values reveal about 350 °C, which is almost the half of the maximum temperature, indicating high thermal stresses inside the tool. As no convective cooling and heat flux into the machine structure is considered, the temperature level might be overestimated. However, the major aim of this work is the development and testing of the workflow. Future studies will adapt the boundary conditions and enhance thermal modeling.

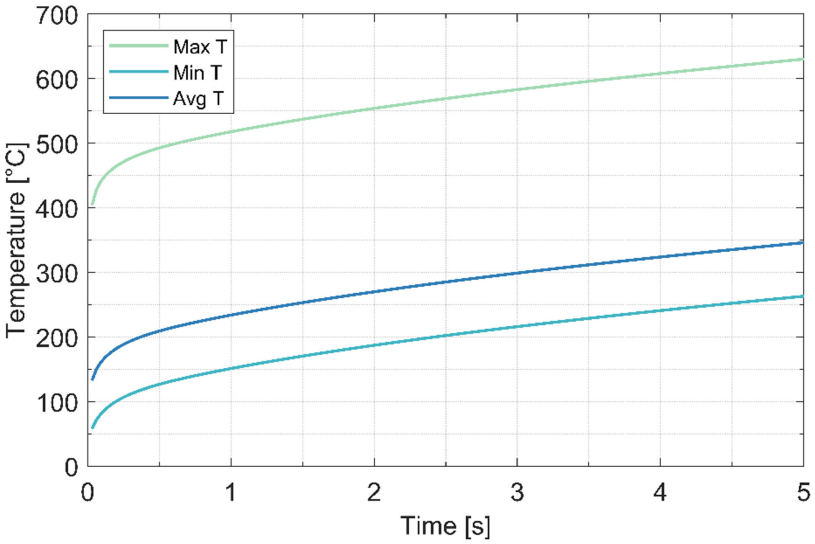

Fig. 7. Minimum, maximum and average temperature during the engagement of one particular cutting edge.

Finally, Fig. 8 investigates the impact of increasing feed rate on the maximum temperature. At the beginning, all three test cases show a similar temperature trend, which starts to deviate after 0.5 s. As expected for higher feed rates, the maximum tool temperature increases. For a feed rate of 3 mm, already after 2 s a maximum temperature of 600 °C is obtained, while for the minimal feed rate twice as much time is required to approach the same niveau. However, particular interesting is that the actual feed rate has no significant impact on the maximum temperature for short milling times. By adding cooling fluid to the process, the deviation from the trends might be shifted to later times.

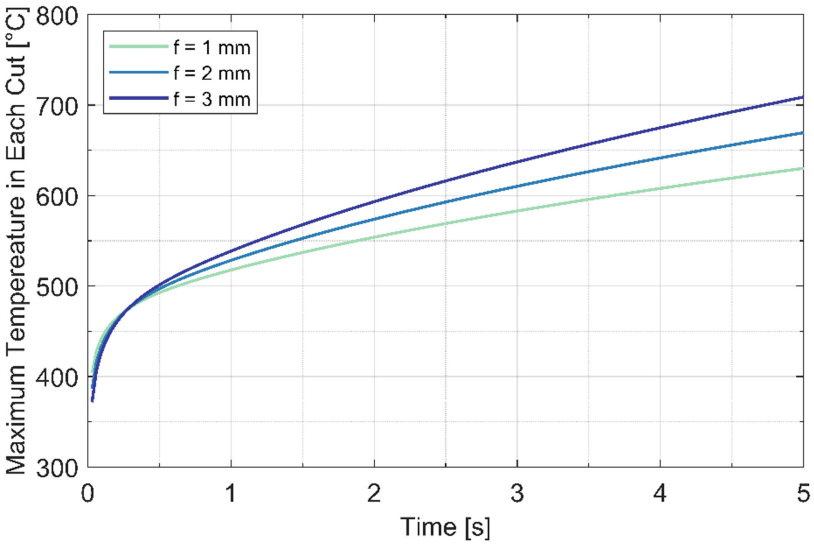

Fig. 8. Maximum tool temperature for three different feed rates.

5 Conclusion

A novel approach to estimate the transient temperature field of a side milling tool has been presented. In a first step, the heat sources are pre-calculated by a FEM simulation and used as a tabulated boundary condition for the later thermal simulation of the milling tool. The thermal model offers to consider transient and spatial varying heat sources during processing. Although time varying heat sources at each cutting edge are considered, the spatial trend is simplified in this work to a constant term. The model shows a physically reasonable results in predicting the transient tool temperature, in particular fast temperature changes at the cutting edge are quantified and can be used in future analysis to estimate thermal induced tool wear and stresses. However, experimental validation is required and will be focused in future research. Further, the thermal model will be enhanced to consider convective cooling by lubricants and contact heat transfer to the workpiece and chip. As significant temperature gradients inside the tool occur, temperature dependent thermophysical properties will also be included.

Acknowledgements. The authors would like to thank the German Research Foundation (DFG) for the funding the SFB/Transregio 96 collaborative research (Project ID 174223256-TRR 96) “Thermo-Energetische Gestaltung von Werkzeug-maschinen” subproject A02 and B02.

References

1. Taylor G.I., Quinney H.: The latent energy remaining in a metal after cold working. In: Proceedings of the Royal Society of London A: Mathematical, Physical and Engineering Sciences. vol. 143, no. 849, pp. 307–326 (1934)
2. Ueda, T., Hosokawa, A., Oda K., Yamada K.: Temperature on flank face of cutting tool in high speed milling. In: CIRP Annals – Manufacturing Technology. vol. 50, no. 1, pp. 37–40 (2001)
3. Sato, M., Tamura, N., Tanaka, H.: Temperature variation in the cutting tool in end milling. J. Manuf. Sci. Eng. **133**(2), 21 (2011)
4. Lin, S., Peng, F., Wen, J., Liu, Y., Yan, R.: An investigation of workpiece temperature variation in end milling considering flank rubbing effect. Int. J. Mach. Tools Manuf. **73**, 71–86 (2013)
5. Jiang, F., Liu, Z., Wan, Y., Shi, Z.: Analytical modeling and experimental investigation of tool and workpiece temperatures for interrupted cutting 1045 steel by inverse heat conduction method. J. Mater. Process. Technol. **213**(6), 887–894 (2013)
6. Karaguzel, U., Bakkal, M., Budak, E.: Modeling and measurement of cutting temperatures in milling. Procedia CIRP **46**, 173–176 (2016)
7. Sölter, J., Gulpak, M.: Heat partitioning in dry milling of steel. Ann. CIRP **61**(1), 87–90 (2012)
8. Lagarde, Q., Wagner, V.: Study of radial depth of cut influence on tool temperature and wear by infrared radiations camera measurements in intermittent cutting. In: Proceeding HSM Metz (2016)
9. Augspurger, T., Meurer, M., Liu, H.: Experimental study of the connection between process parameters, thermo-mechanical loads and surface integrity in machining Inconel 718. Procedia CIRP **87**, 59–64 (2020)
10. Augspurger, T., Bergs, T., Döbbeler, B.: Measurement and modeling of heat partitions and temperature fields in the workpiece for cutting Inconel 718, AISI 1045, Ti6Al4V, and AlMgSi0. 5. J. Manuf. Sci. Eng. **141**(6), 06100 (2019)